PERGAMON

Journal of Atmospheric and Solar-Terrestrial Physics 65 (2003) 901–916

Journal of ATMOSPHERIC AND SOLAR-TERRESTRIAL PHYSICS

www.elsevier.com/locate/jastp

Modeling studies with QBO: II. Solar cycle effect

H.G. Mayr[a,*], J.G. Mengel[b], D.P. Drob[c], K.L. Chan[d], H.S. Porter[e]

[a] Goddard Space Flight Center, MC 910.4 Greenbelt, MD 20771-0001, USA
[b] Science Systems & Applications, Inc. Lanham, MD, USA
[c] Naval Research Laboratory, Washington, DC, USA
[d] University of Science and Technology, Hong Kong, China
[e] Furman University, Greenville, SC, USA

Received 12 November 2001; accepted 2 May 2003

Abstract

Solar cycle activity effects (SCAE) in the lower and middle atmosphere, reported in several studies, are difficult to explain on the basis of the small changes in solar radiation that accompany the 11-year cycle. It is therefore natural to speculate that dynamical processes may come into play to produce a leverage. Such a leverage may be provided by the quasi-biennial oscillation (QBO) in the zonal circulation of the stratosphere, which has been linked to solar activity variations (e.g., Labitzke (J. Meteorol. Soc. Jpn. 60 (1982) 124; Geophys. Res. Lett. 14 (1987) 135); Labitzke and Van Loon (J. Atm. Terr. Phys. 50 (1988) 197; J. Atm. Terr. Phys. 54 (1992) 1453)). Driven primarily by wave mean flow interaction, the QBO period and its amplitude are variable but are also strongly influenced by the seasonal cycle in the solar radiation. This influence extends to low altitudes and is referred to as "downward control". Small changes in the solar radiative forcing may produce small changes in the period and phase of the QBO, but these in turn may produce measurable differences in the wind field. Thus, the QBO may be an amplifier of solar activity variations and a natural conduit of these variations to lower altitudes. To test this hypothesis, we conducted experiments with a 2D version of our numerical spectral model that incorporates Hines' Doppler spread parameterization for small-scale gravity waves (GW). Solar cycle radiance variations (SCRV) are accounted for by changing the radiative heating rate on a logarithmic scale from 0.1% at the surface to 1% at 50 km to 10% at 100 km. With and without SCRV, but with the same GW flux, we then conduct numerical experiments to evaluate the magnitude of the SCAE in the zonal circulation. The numerical results show that, under certain conditions, the SCAE is significant and can extend to lower altitudes where the SCRV is small. For a modeled QBO period of 30 months, we find that the seasonal cycle in the solar forcing acts as a strong pacemaker to lock up the phase and period of the QBO. The SCAE then shows up primarily as a distinct but relatively weak amplitude modulation. But with a different QBO period between 30 and 34 (or < 30, presumably) months, the seasonal phase lock is weak. Solar flux variations in the seasonal cycle then cause variations in the QBO period and phase. These amplify the SCAE to produce relatively large variations in the wind field. The SCAE in this case extends to mid-latitudes.

Keywords: Solar cycle effect; Quasi biennial oscillation; Middle atmosphere dynamics; Gravity waves; Atmospheric model

1. Introduction

Following a study by Holton and Tan (1980) that revealed an influence of the phase of the quasi-biennial oscillation (QBO) on the dynamics of the stratosphere, Labitzke (1982, 1987) and Labitzke and Van Loon (1988, 1992) discovered that the temperatures at northern polar latitudes in winter are positively and negatively correlated with the solar cycle activity when the QBO was in its negative and positive phase, respectively. At mid-latitudes they observed opposite correlations. Naito and Hirota (1997) confirmed these findings. In the northern stratosphere and for the period between 1964 and 1994, Dunkerton and Baldwin (1992) and Baldwin and

* Corresponding author.
E-mail address: hmayr@pop900.gsfc.nasa.gov (H.G. Mayr).

1364-6826/03/$ - see front matter
doi:10.1016/S1364-6826(03)00111-1

Dunkerton (1998) found evidence of a quasi-decadal oscillation correlated with the QBO and solar cycle. Signatures of such a decadal oscillation have also been reported by Van Loon and Labitzke (1993, 1998) based in part on data going back almost 40 years.

A GCM modeling study by Balachandran and Rind (1995) found general agreement with the above observations. They also found that their model produced a significant solar activity effect in the troposphere. Balachandran et al. (1999) later extended this study and found during solar maximum, in agreement with observations, a significant increase of geopotential heights that is correlated with the phase of the QBO. They attributed their results to the changing vertical and horizontal gradients of zonal winds and temperature, respectively, that are produced by the changing solar radiation. These geopotential height changes then alter the propagation conditions for planetary waves, which in turn affects the circulation at lower altitudes.

From the above results it is not clear what role the QBO is actually playing in the solar activity effects that have been reported. The QBO, and its phase in particular, may act as a catalyst to change the propagation conditions for waves and bring about the observed solar cycle activity connection. But the QBO itself may also be affected directly by the solar cycle (Salby and Callaghan, 2000; Soukharev and Hood, 2001)—and this is the avenue we are examining in the present paper. In an accompanying paper (Mayr et al., 2001, Part I), we show how the QBO can generate quasi-decadal oscillations through interactions with the seasonal variations.

As discussed also in Part I, the QBO (with periods between 22 and 34 months) is confined to low latitudes where it dominates the zonal circulation of the lower stratosphere (Reed, 1965, 1966), but it is also observed in the upper mesosphere (Burrage et al., 1996). Closely connected with the QBO is the semi-annual oscillation (SAO), which dominates the equatorial circulation of the upper stratosphere and mesosphere (Hirota, 1980). Momentum deposition by planetary waves can in principle explain the stratospheric oscillations. This was demonstrated by Lindzen and Holton (1968), Holton and Lindzen (1972) and others (e.g., Plumb, 1977; Plumb and Bell, 1982; Plumb, 1984; Dunkerton, 1985) for the QBO, and by Dunkerton (1979) and Hamilton (1986) for the SAO that in turn strongly interacts with the QBO (e.g., Dunkerton and Delisi, 1997; Garcia et al., 1997). Upward propagating planetary waves cannot reach the upper mesosphere with sufficient amplitudes, but small-scale gravity waves (GW) can provide the momentum source required to generate the SAO at these altitudes (Dunkerton, 1982a). Modeling studies with observed planetary waves have lead more recently to the conclusion that GWs are also required for the stratosphere (e.g., Hitchman and Leovy, 1988; Takahashi and Boville, 1992; Hamilton et al., 1995). Except for the QBO simulation with a GCM by Takahashi (1999) that was capable of resolving GWs, these waves normally need to be parameterized for global-scale models. Following Lindzen (1981), a number of such schemes have been developed (e.g., Dunkerton, 1982b, c; Fritts and Lu, 1993). Dunkerton (1997) employed a GW parameterization to successfully simulate the QBO in the stratosphere. We shall employ the Doppler spread parameterization (DSP) of Hines that has allowed us to simulate the QBO and SAO extending from the lower stratosphere into the upper mesosphere (e.g., Mengel et al., 1995; Mayr et al., 1997).

2. QBO, downward control, and period modulation

In the theory of Lindzen and Holton (1968), the seasonal cycle and resulting SAO were invoked to seed the wave-driven QBO. Holton and Lindzen (1972) subsequently concluded that the seasonal cycle, while important, is not essential to generate this kind of oscillation. Owing to this generation mechanism for the QBO, i.e., driven by waves but influenced also by solar heating, the QBO can transfer the effect of solar cycle radiance variations (SCRV) to lower altitudes. Two factors are important.

First, waves can efficiently generate the QBO at equatorial latitudes because, with the Coriolis force vanishing, the meridional circulation is not involved in the redistribution of equatorial wave momentum. The momentum that drives the QBO remains trapped near the equator where it is transferred through the wave interaction to lower altitudes, referred to as “downward control”.

Second, as pointed out above, the QBO is influenced by the seasonal variation in the solar radiative forcing, which was demonstrated explicitly in computer experiments (Mayr et al., 1998, see Figs. 1 and 2). In that paper, Fig. 1 shows the equatorial oscillations generated with the seasonal cycle of solar heating and Fig. 2 shows them for comparison with constant solar heating at perpetual equinox. The seasonal cycle causes in the QBO a significant increase in amplitude from 3 to 7 m/s at 30 km and increases its period from about 17 to 21 months. The computed amplitude of the dominant oscillation at higher altitudes also increases, but its period decreases from 8 to 6 months to produce the SAO that is phase locked to the seasonal cycle (with the Sun crossing the equator twice a year).

In summary, the momentum deposited by upward propagating waves that drives the equatorial QBO is trapped and transferred, partially through diffusion, to lower altitudes. This process is modulated by the seasonal variations in the solar heating of the mesosphere where the solar cycle influence can be important, to exert downward control by partially seeding the QBO. Through the seasonal cycle, long-term SCRV then can influence the amplitude and period of the QBO. By changing the period of the QBO in particular, and through downward control, the SCRV can thus exert leverage on the SCAE at lower altitudes.

Based on our analyses, two other processes are of interest in the context of QBO related solar activity effects. One is the synchronization of the QBO by the seasonal cycle of solar forcing. As mentioned earlier, the other one involves the QBO to produce beat periods around 10 years, which are generated through interaction with the seasonal cycles and GW node filtering.

In this modeling study we shall show how the QBO can get involved in amplifying the solar activity effect: (a) as a conduit of the solar activity effect to lower altitudes, (b) through period modulations of the QBO, and (c) through amplitude modulations of the seasonal variations. We shall make use of spectral analysis to reveal in some detail these signatures of solar activity in the model. The purpose is, and we emphasize this, to provide an understanding of the generic processes involved. Since the 2D model applied here is not sufficiently realistic to provide meaningful predictions, we realize that our analysis is thus merely of academic interest at best.

Referring to Part I, we shall briefly describe our model and define the gravity wave parameters that are employed to drive the circulation. We shall then present the results from computer experiments for QBOs with periods of about 30 and 33 months, for which the SCAEs are vastly different owing to the importance of period modulation relative to amplitude modulation.

3. Numerical model

The computer experiments presented here use a 2D version of our numerical spectral model (NSM) whose numerical design was discussed by Chan et al. (1994). As discussed in Part I, the model is time dependent and non-linear, and it is driven by solar UV radiation absorbed in the stratosphere and mesosphere (Strobel, 1978) and by EUV radiation absorbed in the thermosphere. The radiative energy loss is formulated in terms of Newtonian cooling, which affects the period of the QBO significantly.

To simulate SCRV perturbations in the atmosphere, we adjust the model's internal heating rates using the simple scheme illustrated in Fig. 1. We assume that the solar radiative heat source varies with the solar cycle on a logarithmic scale by 0.1% at the surface, 1% at 50 km, and 10% at 100 km and above. The variations below 30 km, however, are irrelevant since the model only accounts for solar heating due to UV and EUV radiation in the stratosphere, mesosphere and thermosphere. Above 100 km, the observed solar radiance variations are much larger but are assumed to have negligible influence on the atmospheric perturbations in the middle atmosphere.

The DSP for GWs, developed by Hines (1997a,b), provides the wave momentum source and the related vertical eddy diffusivity due to wave-driven turbulence. The wave momentum flux is proportional to $\sigma_h^3 k_*$, where σ_h is the GW horizontal wind variability, and k_* is the characteristic horizontal wave number. For simplicity, these parameters are taken to be globally uniform and independent of season. The GW source is initiated at the surface, with the momentum flux taken to be isotropic in the four cardinal directions.

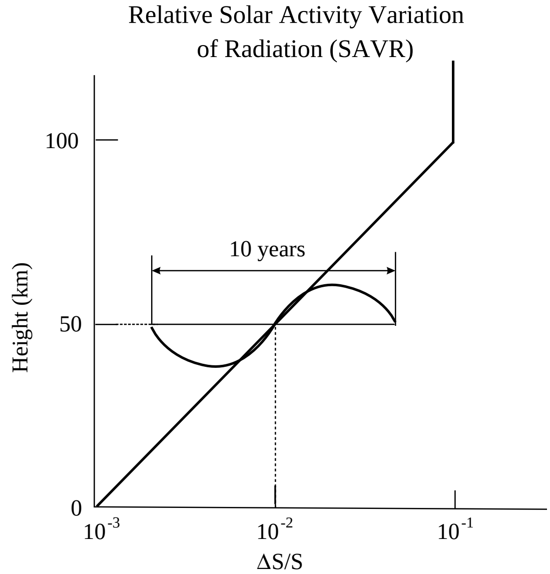

Fig. 1. Schematic, illustrating the adopted height variation of the relative solar activity variation in the heating rate on a logarithmic scale. For comparison, model results will also be shown for a 3 times larger amplitude and with an activity cycle of 8 years.

4. Case studies for QBO-related solar activity effects

The purpose of this study is to elucidate a dynamical mechanism that involves the QBO and may contribute to amplify the SCAE in part by coupling the mesosphere to the stratosphere and even troposphere and by coupling the atmosphere at mid latitudes to the tropics. We ask whether the equatorial oscillations, and in particular the QBO, could bring about an amplification of the SCAE through downward control. Addressing this question, two case studies are presented. The first describes a hypothetical QBO with an average period of 30 months that is phase locked to the seasonal variations. The second study deals with a hypothetical case where the average QBO period is about 33 months, which is near the upper end of observed periodicities. In the first case, the SCAE is significant but relatively small, and it appears primarily as an amplitude modulation of the QBO. In the second case, the SCAE is much larger and is accompanied by phase variations of the QBO.

4.1. Case study 1 with 30-month QBO

With a period of 30 months, the phase condition is optimally satisfied for the QBO to be synchronized by the semiannual variations (e.g., Mayr et al., 2000). Under this condition, the seasonal cycle acts as a strong pacemaker for the QBO. To produce this 30-month QBO, we chose the

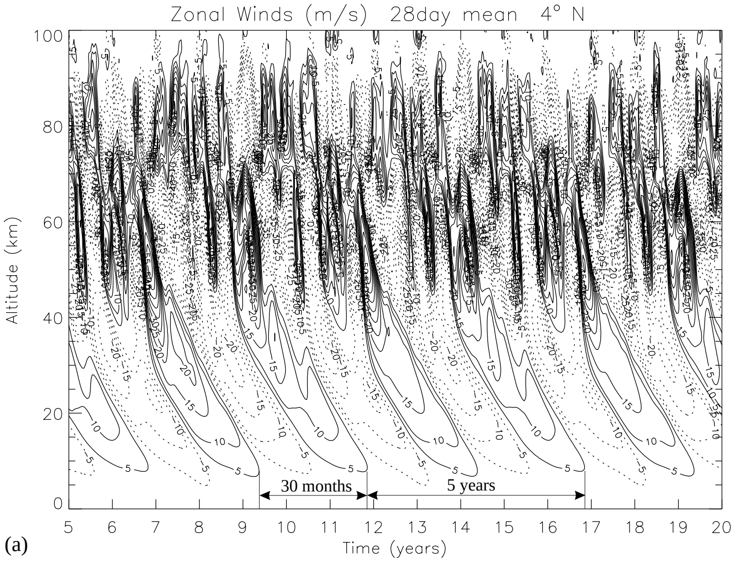

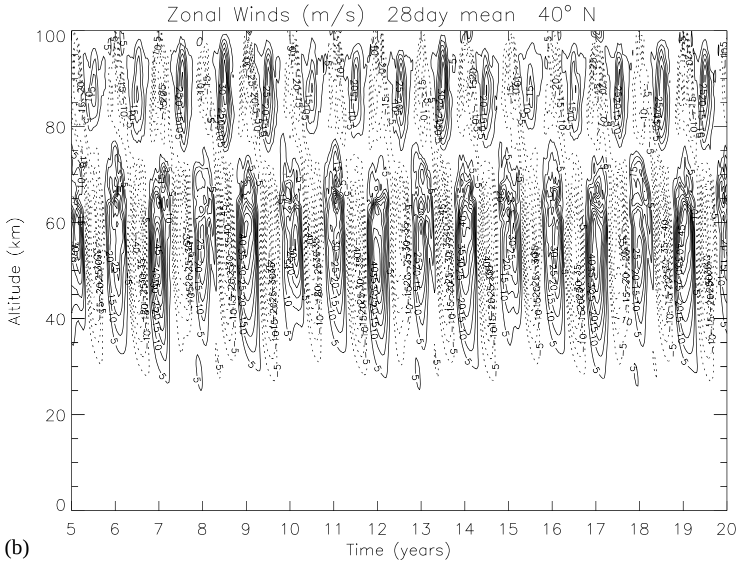

Fig. 2. Computed zonal winds at latitudes 4° (a) and 40° (b) for case 1. With a period of 30 months, this QBO is strongly tied to and synchronized by the SAO to produce an exceptionally stable oscillation (Mayr et al., 2000). Such a QBO interacts with the (AO) to generate a beat period of 5 years through GW node filtering.

GW parameters to be $k_* = (120\ \mathrm{km})^{-1}$ and $\sigma_{\mathrm{hi}} = 3$ m/s at 20 km. The cooling rates from Wehrbein and Leovy (1982) are adopted.

Allowing for sufficient spin-up time, we present in Fig. 2 the results from the standard computer run obtained without imposing the SCRV. The computed monthly mean zonal winds are shown at 4° and 40° in the northern hemisphere. Two related features are of particular interest. Firstly, the QBO at 4° latitude is modulated with a beat period of 5 years (Mayr et al., 2000), also shown in the subsequent Figs. 3 and 4, which is generated through GW node filtering by interaction with the annual oscillation (AO). Secondly, at low latitudes, the signature of the AO-induced beat period extends down to 10 km, while at mid latitudes the AO itself is confined to altitudes above 30 km where it dominates.

These features are delineated in more detail in the spectrum of the zonal winds at 4° latitude that is shown in Fig. 3 for a time span of 30 years. The spectrum is presented in terms of the harmonics, h, with the associated periods determined by 30/h (in years) in this case. Separately, the hemispherically symmetric (a) and anti-symmetric (b) components are shown; and the dominant lines for the symmetric

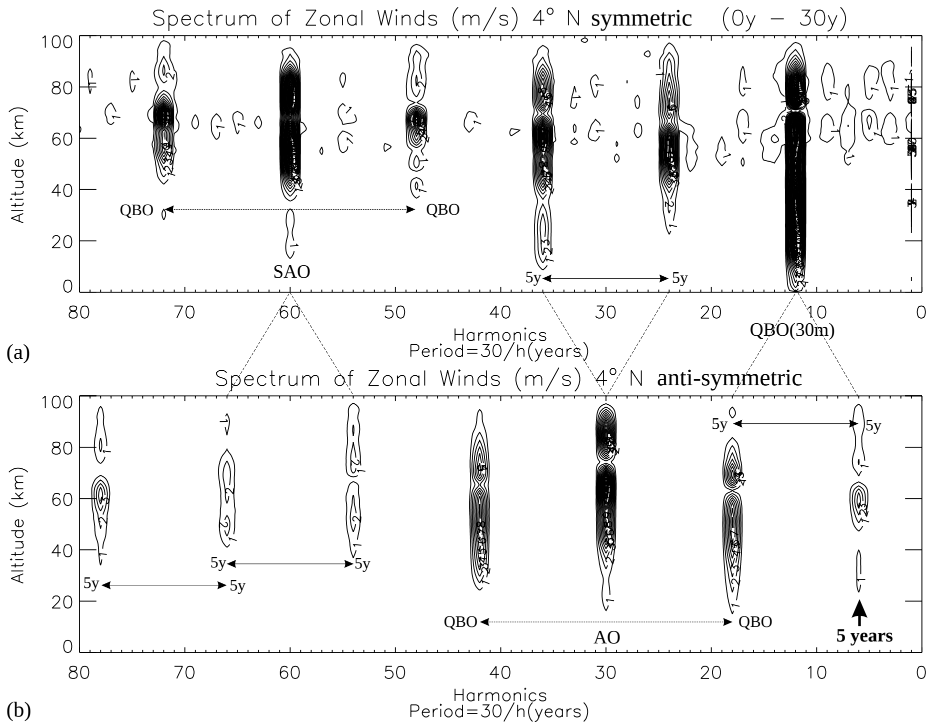

Fig. 3. Spectrum of the equatorial oscillations in the zonal winds at 4° north (as seen in Fig. 2) obtained from a solution spanning 30 years beginning at a time the atmosphere was spun up. The spectrum is presented in terms of harmonics, *h*, that are related to periods by 30/h (years) in this case. Hemispherically symmetric (a) and anti-symmetric (b) components are shown, and the various "spectral lines" are identified. The 5-year beat is hemispherically anti-symmetric being generated by the symmetric QBO and anti-symmetric AO. Due to quadratic non-linear interactions (i.e., AxB), in part due to GW phase filtering, the identified "side lobes" (or lobe harmonics) are generated—and they are all tied to the QBO directly or indirectly. The rich phenomenology revealed in the spectrum, and apparent in Fig. 2a, is thus to a large extent caused by the QBO and the wave interactions it involves.

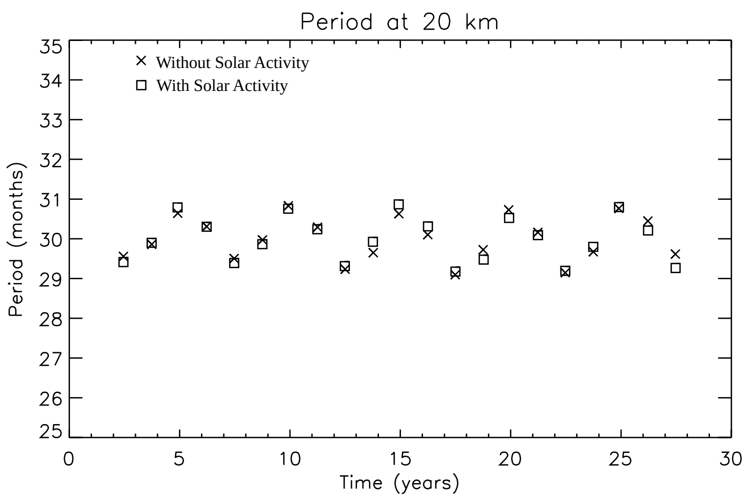

Fig. 4. Period at 4° north and at 20 km altitude obtained from intervals between times the computed zonal winds change direction. This is considered to be the period of the QBO, which dominates at this altitude. Note in this case that the variations around 30 months are fairly regular and thereby reveal the 5-year beat period. Also presented is the QBO period obtained from a solution with SCAV, illustrated in Fig. 1, which does not show a discernable effect.

QBO and SAO and anti-symmetric AO are identified. Also identified is the anti-symmetric 5-year beat period, which is produced by the symmetric QBO interacting with the anti-symmetric AO. While the 5-year beat period at $h = 6$ is relatively weak, it is more pronounced in the side-lobes (harmonics) that identify quadratic non-linear interactions with the QBO ($h = 12 \pm 6$), the AO (30 ± 6), and SAO (60 ± 6). Unlike the 5-year beat period, which is generated above 40 km, these modulations extend to lower altitudes with much larger amplitudes. This illustrates the importance of downward control at low latitudes, as discussed in greater detail in Part I. All the other features in the model spectrum can also be readily explained in this particular case and accordingly are identified. Except for the AO and SAO, all the spectral lines are shown to be related to the QBO.

When we run the model with the solar activity variations illustrated in Fig. 1, the resulting zonal wind field at low latitudes is different from that shown in Fig. 2a. The resulting changes, however, are not large enough to identify an obvious solar activity signature. We therefore take the approach of examining the difference fields instead. One of the quantities to compare is the period of the QBO, which is determined from the time spans between points the winds change direction. This QBO period is presented for model runs with and without solar activity variations in Fig. 4 for the 20-km altitude at 4° latitude. It shows that the QBO period varies around 30 months, and the variations clearly reveal the 5-year beat period that is generated by the interaction with the AO. The differences between the solutions with and without solar activity, however, are slight. As pointed out earlier, in this particular case, the AO acts as a strong pacemaker to lock the period of the QBO—which is by no means typical as the second case study will show where the variations are less regular, and the solar activity-related differences between the QBO periods are much larger.

In Fig. 5a we show for 4° latitude the yearly average of the differences between the zonal winds computed without and with solar activity variations. The pattern seen here clearly reveals the 10-year periodicity imposed by the solar activity cycle, but the signal is not as clean as one would have liked to see. The tongues that extend down to lower altitudes around the year 5 are also there around the year 15, but they are split up around the year 25. At altitudes above 70 km, the zonal wind differences tend to be out of phase with those below and again reveal the imposed 10-year solar activity cycle. Considering that the assumed relative solar activity variations vary from 1% to 10% between 50 and 100 km, respectively, the resulting zonal wind differences of about 10 m/s at around 60 km are large. But the effect does not grow proportionally with altitude, which suggests that the amplification is tied to the stratospheric QBO and that the signatures in the upper mesosphere are produced by the filtering of upward propagating GWs.

To gain further insight we ran the model also with a factor-of-three increase in the solar activity variations relative to those shown in Fig. 1. For the QBO period, the differences are slightly larger compared to Fig. 4, but the differences are not large enough to be significant. The differences in the zonal winds, shown in Fig. 5b, however are significant. Compared with Fig. 5a, the phases of the zonal wind differences (i.e., patches of positive and negative values) are in general agreement, as one should expect from the identical phasing of the adopted solar cycle variations. The wind differences are also larger during the first 10-year cycle, and they extend to lower altitudes. During the second cycle, however, the wind differences are smaller, and they are confined to altitudes above 50 km. During the third cycle, there is again a tendency for the perturbations to increase in magnitude and to extend to lower altitudes. Overall, however, the factor of three increase of the SCRV does not produce a corresponding increase in the difference field. This reveals one of the difficulties in our understanding of the underlying processes, which are inherently non-linear.

The picture is somewhat clearer, when the zonal wind differences are presented in spectral notation as shown in Fig. 6 for the symmetric components (the contour interval is 0.5 m/s, and the minimum value is chosen to be 1 m/s). For both solar activity levels, the 10-year harmonic, $h = 3$, stands out along with the solar activity modulation of the QBO that is identified. With increased SCAV, the amplitudes are noticeably enhanced. Notable differences are seen in the 10-year QBO modulation ($h = 12 \pm 3$) that sharpens with enhanced activity. With 3x SCAV, prominent features appear also at (33, 39), which can be related to one of the side-lobes at $h = 36$ shown in Fig. 4 that in turn is produced by the modulation of the AO with the 5-year beat period. Similarly, the features at (69, 75) may be related to one of the side-lobes at 72 shown in Fig. 4 that is produced by the modulation of the SAO with the QBO. Most of the features in the difference spectrum that appear only in the solution with 3x SCAV thus can be traced to complicated dynamical interactions involving the AO and SAO— and this explains in part the above discussed differences between Figs. 5a and b.

With the spectra shown in Fig. 6, we can synthesize the dominant lines to create filtered pictures of the difference fields. These are shown in Fig. 7a and b for the two levels of SCRV. For comparison, we employ in both cases the same prominent harmonics: $h=3$ for the 10-year solar cycle, and $h = 9$ and 15 for the 10-year side-lobes of the QBO. These synthesized difference fields thus describe the filtered first-order SCAE for this particular QBO. Not surprisingly, the features that appeared in Fig. 5a also appear in Fig. 7a, since the chosen harmonics essentially describe the bulk of the difference field. The same cannot be said for Figs. 5b and 7b, because the adopted spectral lines describe there only a subset of the computed difference field. For the filtered difference field, however, the 10-year amplitude modulation increases significantly with increased SCRV, as expected, and the effect extends to lower altitudes.

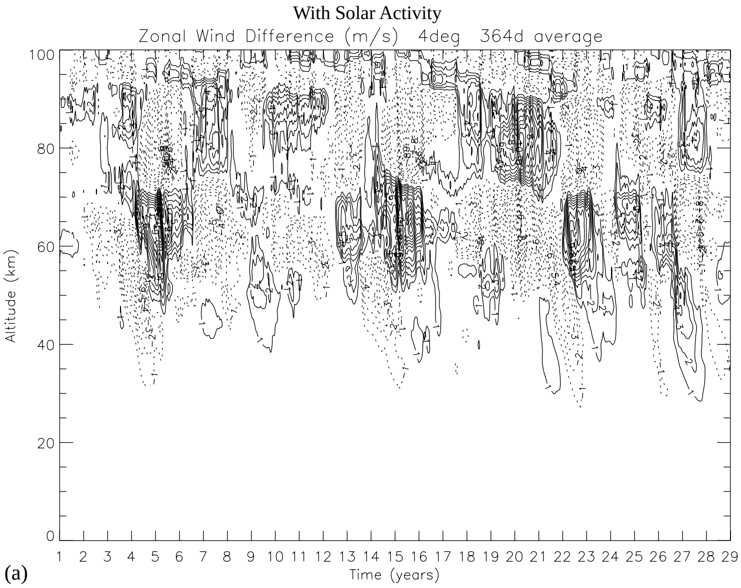

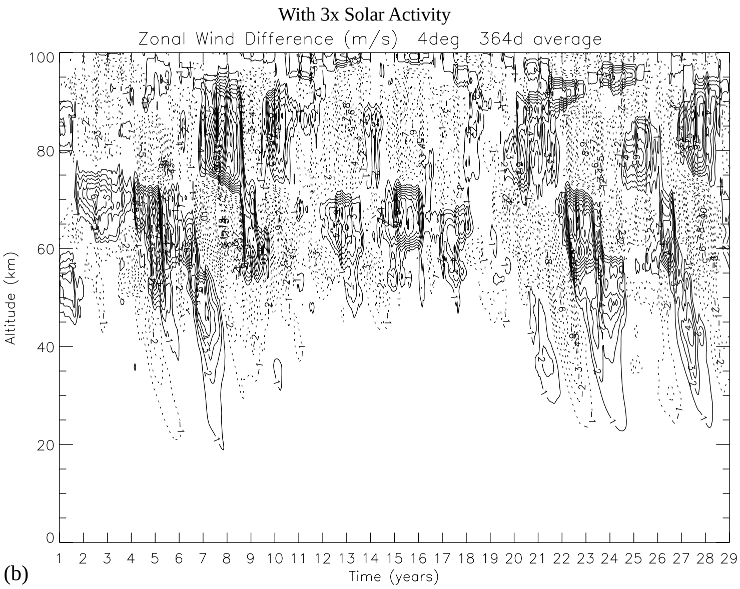

Fig. 5. Computed differences of zonal winds at 4° north obtained by subtracting solutions with solar activity variations from a solution without solar activity. The difference field (a) is obtained by employing the standard SCAV shown in Fig. 1, while for (b) the adopted SCAV is 3 times larger. In both cases, the difference fields reveal the 10-year periodicity of solar activity. GW filtering apparently causes the phase reversals at altitudes above 70 km. The factor of 3 increase in solar activity does not produce a corresponding increase in the difference field, but it shows some tendency for the effect to extend to lower altitudes.

In summary, we have seen from this case study that the SCAE is confined to low latitudes where it shows up as an amplitude modulation of the QBO. In this instance, the QBO is being synchronized by the seasonal cycle so that its period and phase become tightly locked. The situation is thus unusual, but it provides a valuable reference for the next case study, where the QBO is more variable, and the SCAE is larger.

4.2. Case study 2 with 33-month QBO

For the hypothetical 33-month QBO, the model runs covered 50 years. The GW parameters were taken to be $k_* = (65\ \mathrm{km})^{-1}$ and $\sigma_{\mathrm{hi}} = 3$ m/s at 20 km to produce about a factor of 2 larger momentum flux, but the adopted eddy diffusion rate was also almost a factor of 2 larger to assure numerical stability. In this case, we adopted the more

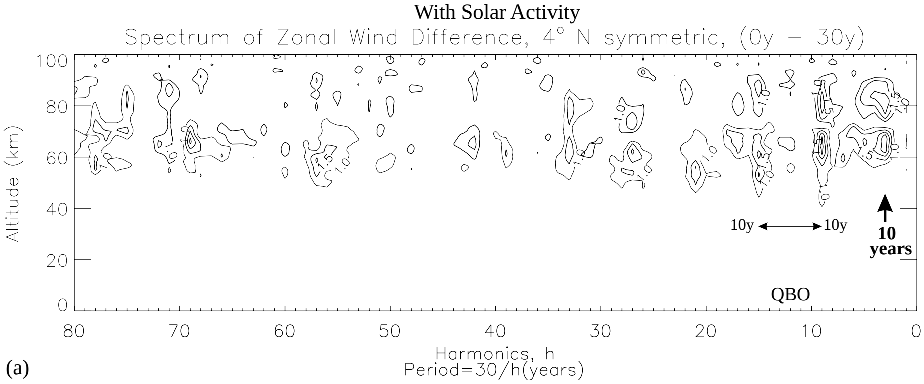

(a)

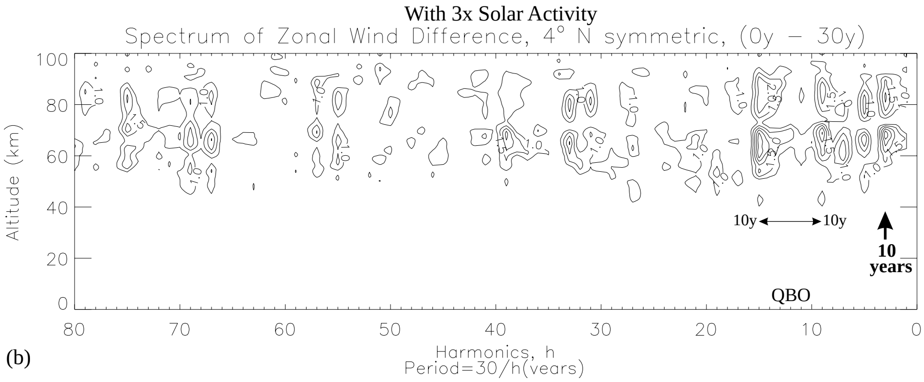

(b)

Fig. 6. Spectra for a 30-year time span of the symmetric components of the difference fields in Fig. 5, shown with 0.5 m/s contour intervals and the lowest contours at 1 m/s to suppress chaff. The 10-year activity cycle is evident for the nominal SCAV (a) at $h=3$ and is significantly stronger when it is enhanced (b). This is also evident in the side-lobes $h = 12 \pm 3$ that describe the amplitude modulation of the QBO, which itself is not apparent in the difference fields. The spectral features in (b) at (69, 75) appear to be related to the 10-year modulation of the QBO (9,15) that in turn can modulate the SAO (60). But the harmonics at (5,7) in (b) cannot be readily explained.

recent cooling rates provided by Zhu (1989). Additionally, the numerical experiments were performed using a shorter integration time step of less than 5 min.

The QBO for this case study is discussed in Part I as an example to illustrate how it can generate a hemispherically symmetric quasi-decadal oscillation that results from an interaction of the QBO with the SAO through GW node filtering. We refer to Fig. 7 of Part I, where we present at 4° N the computed zonal winds averaged over a year. The period of the QBO is on average 33.5 months. Repeatable features indicate a modulation with a period around 10 years, but the pattern is not as clean as that for the 5-year beat period seen in Fig. 2. As Fig. 9 of Part I shows, the amplitude modulation of the zonal winds are large at 40°N. During the first cycle, the modulation period is close to 11 years, but for the second cycle it is closer to 9 years. Apparently, the beat period is fluctuating around 10 years, and this adds a potential complication when SCRV with such a duration are employed.

Analogous to Fig. 4, we present in Fig. 8 the variations of the periodicity of the zonal winds at 20 km computed with and without SCRV. Because of the conflicting 10-year beat period that comes into play in this case, the model was also run with a hypothetical solar cycle period of 8 years (b). In contrast to Fig. 4 for the 30-month QBO that is phase locked to the seasonal cycle, the periodicity in Fig. 8 is highly variable without revealing any discernable patterns. The same is true for the solutions with SCRV, which differ also significantly for the two different periodicities (10 and 8 years) chosen.

That the QBO period in this case, and in general, is variable is not surprising. Waves propagating up are filtered by the QBO and as a result influence the AO and SAO, as the spectral lines in Fig. 3 illustrate that tie these components together. On the other hand, we have also seen that the AO and SAO, influenced by the QBO, in turn influence the QBO even to the extent that it can act as a strong pacemaker to produce a phase lock in the previous case study (e.g., Fig. 4). The two interactions, transferring momentum both upwards and downwards, are strongly non-linear due to the importance of feedback processes. This in turn introduces into the dynamical system a significant quasi-chaotic component, which is difficult to unravel.

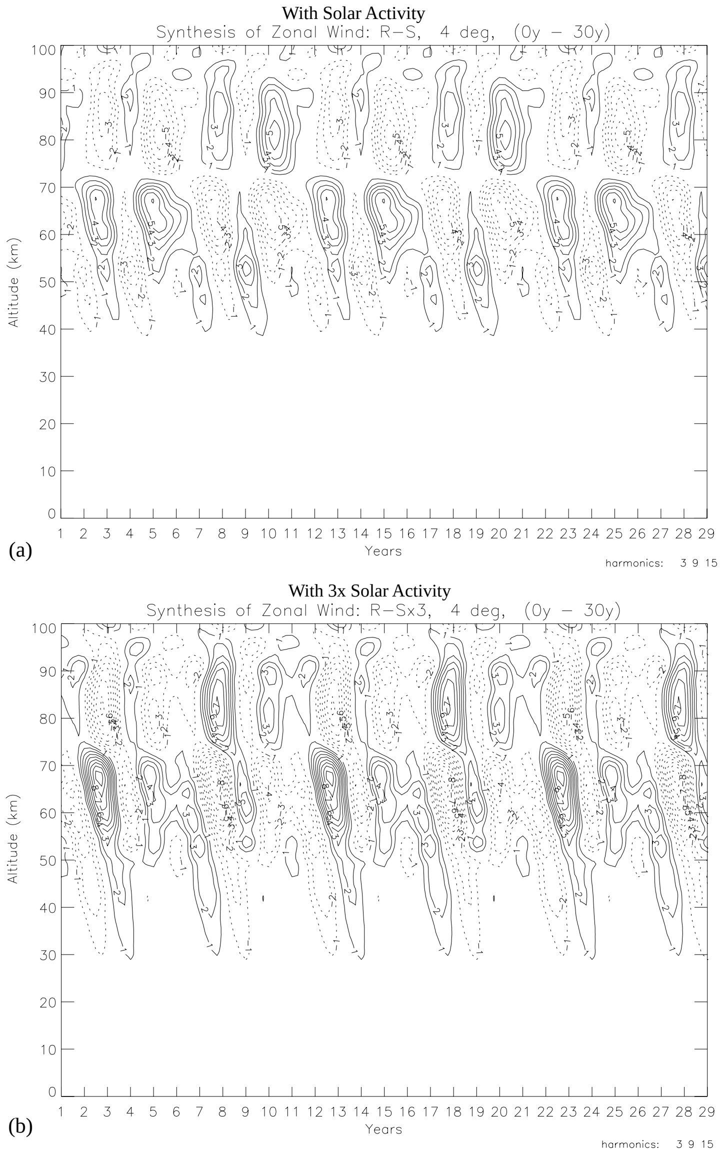

Fig. 7. Syntheses of the harmonics $h = 3, 9, 15$, which are prominent in Fig. 6. This reveals the 10-year modulation of the QBO. For (a) it resembles also the difference field shown in Fig. 5a as expected. For (b) the resemblance with Fig. 5b is less obvious because that spectrum contains prominent features not accounted for in the synthesis. But it does show a significant increase in the modulation amplitude commensurate with the enhanced activity.

In this particular case. the effect is dramatic when the model is run with SCRV. With the 10-year activity cycle, the phase of the QBO gradually changes so that after about 7 years the polarity (sign) of the oscillation is reversed. The oscillation then continues in this phase for the remaining 40 years of the numerical experiment. This is shown in Fig. 9a for the difference field, with contour intervals of 10 m/s, reaching magnitudes almost twice as large as those shown for the original wind field (Fig. 7 of Part I). The phase variations introduced by the 10-year solar activity cycle drives the atmosphere into another state that is commensurate with, and becomes locked to, the natural beat period of 10 years. Apparently, this is caused by the coincidence of the beat and activity periods.

As mentioned earlier, to avoid this coincidence, the model was also run with a hypothetical 8-year activity cycle. The result for the difference field is presented in Fig. 9b with contour intervals of 5 m/s. In this case, the oscillation at

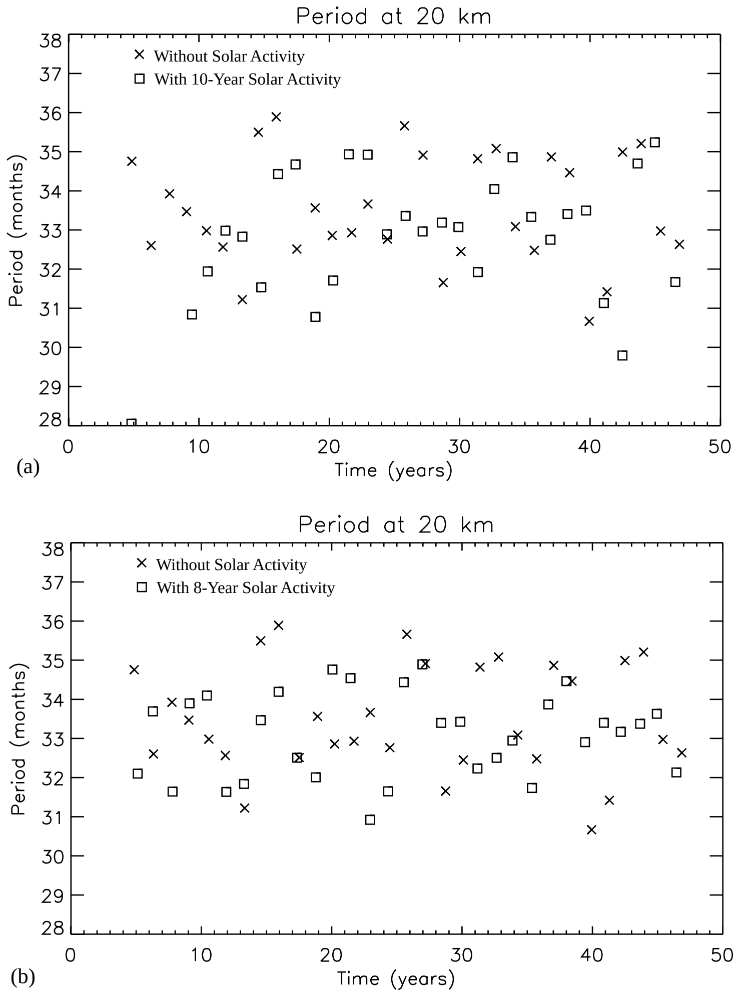

Fig. 8. QBO periods at 4° north and at 20 km altitude obtained for case 2 from intervals between times the computed zonal winds change direction. Results are presented for fictitious solar activity cycles of 10 years (a) and 8 years (b). In contrast to Fig. 4, large and irregular variations occur that do not reveal the beat period or any other obvious pattern. Deviating from Fig. 4 also, the differences between QBO periods with and without solar activity are relatively large.

altitudes below 30 km also builds up but much later after more than 25 years, and the velocities do not come close to those generated in Fig. 9a. In contrast to the previous case, the activity cycle is not synchronized with the beat period. On the other hand, the results show that the difference field is not dominated by a period of 8 years either but one that is closer to 10 years, which suggests that the beat period continues to play a significant role.

To provide more insight, we present in Fig. 10a for 4° N the spectra computed from a 40 year time span of the difference fields (with 1 m/s contour intervals starting at 3 m/s). Along with the 10-year signal of the activity cycle at $h = 4$ and its second harmonic at $h = 8$, the figure shows the large QBO amplitude that results from the phase reversal discussed above. The other prominent features in the spectrum are associated with the AO and SAO, although these are not present in the difference field as expected. As indicated, the anti-symmetric side-lobes $h = 40 \pm 4$ are caused by the 10-year modulation of the AO, and the features at (40 ± 14) result from the QBO modulation of the AO. Similarly, the symmetric harmonics at (80 ± 4) are generated by the 10-year modulation of the SAO, and (80 ± 14) results from the QBO modulation of the SAO. Among the remaining features, the symmetric harmonics (62, 98) appear to be generated by the 10-year modulation of the QBO that in turn modulates the SAO as indicated. The same pattern is also apparent in the anti-symmetric harmonics (22, 58) that reveal the corresponding interactions with the AO. While these spectral features convey understanding and some confidence in the model results by

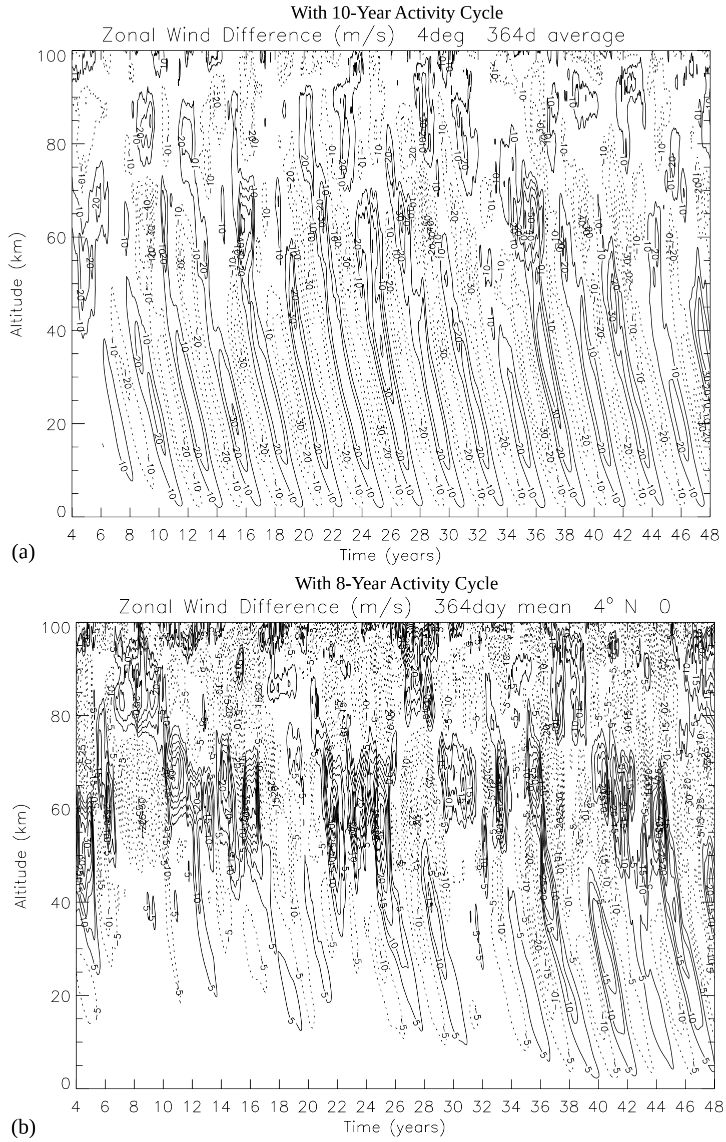

Fig. 9. Computed zonal wind differences at 4°, similar to Fig. 5, obtained for the two activity cycles. Note the large differences in (a), with contour intervals of 10 m/s, which develop after about 7 years due to a gradual shift in the phase of the QBO. Apparently, the 10-year activity cycle becomes synchronized with and phase locked to the 10-year beat period. In contrast to that, the differences for the 8-year activity cycle in (b), with contour intervals of 5 m/s, are much smaller. But eventually after 25 years the phase shift produces large differences in the QBO at lower altitudes. In (b), pronounced differences are apparent, with periods near 10 years and amplitudes as large as 20 m/s, much larger than those in Fig. 5.

implication, they also reveal the complex nature of possible interactions.

For the 8-year activity cycle presented in Fig. 10b, the spectrum contains many of the same features discussed above. The QBO signatures are also present in this simulation but are much weaker than those seen in Fig. 10a. The signal of the activity cycle is seen in the 10-year harmonic (4), which is accompanied by a strong feature at 6 that corresponds to a period of about 6.7 years and may indicate a shift towards 8 years. We note the spectral features (10, 18) that reveal the 10-year modulation of the QBO. The SCRV related harmonics at $h = 4, 6, 8$ apparently create amplitude modulations of the AO and SAO.

Unlike in the first case study for the phase locked QBO, the SCAE in the difference field now extends to higher latitudes as shown in Fig. 11. Distinct SCAE signatures are

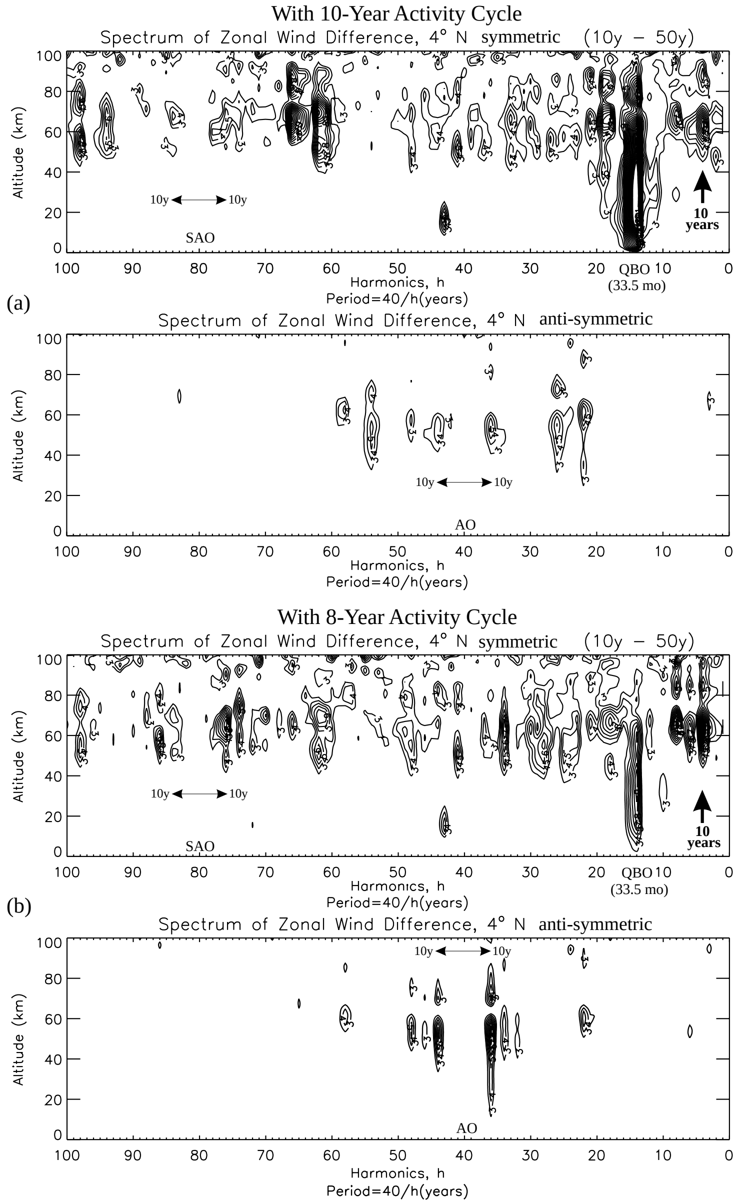

Fig. 10. Spectra for 40-year time spans (10–50 model years) of the difference fields of case 2, shown with 1 m/s contour intervals and the lowest contours at 3 m/s to suppress chaff. The periods are now related to the harmonics, h, by 40/h (years). Commensurate with Fig. 9, the QBO feature dominates in (a), but the AO and SAO (firmly tied to the seasonal forcing) are eliminated by differencing. The 10-year activity cycle and its second harmonic are pronounced at $h = 4$ and appear in the side-lobes of the AO and SAO. Also shown, though fussy, are the corresponding side-lobes for the QBO. The pronounced features at (66, 94) describe the modulation of the SAO by the QBO, and the ones at (62, 98) in turn are consistent with the resulting modulation by the activity cycle. Similar features are also evident for the 8-year cycle in (b), except that the QBO signature is much weaker. In addition to the harmonic at 4 for the 10-year periodicity, a pronounced one occurs also at 6 that corresponds to a period of about 6.7 years, indicating a shift towards the imposed 8-year activity cycle.

seen here, with differences in the wind field of ±10 m/s that reveal periodicities around 10 years. The pattern though is less pronounced for the 8-year cycle below 60 km, which suggests a conflict between the imposed activity variation and the inherent 10-year beat period. There is no significant difference between the amplitudes of the difference fields in both cases, which is surprising considering the large differences seen at low latitudes (Fig. 9).

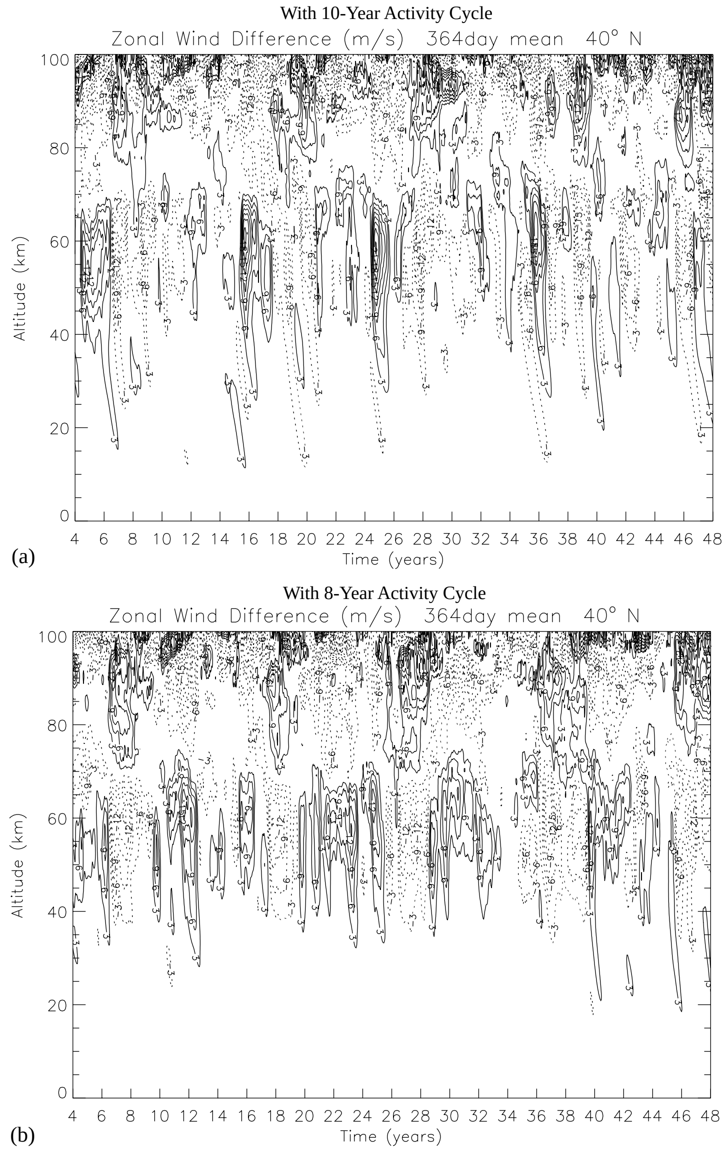

Fig. 11. Difference fields at 40° latitude for the 10- and 8-year activity cycles. Periodicities around 10 years are seen in the wind fields, and the amplitudes are on the order of 10 m/s in both cases.

5. Summary and conclusion

In the modeling study presented here, we have explored a dynamical mechanism that may conspire to enhance the solar cycle activity effect SCAE through the QBO. Although generated primarily by wave mean flow interaction, the amplitude and period of the QBO are affected by the seasonal cycle of solar forcing. Our hypothesis is that the SCAE could then result not so much from an amplitude modulation of the QBO but from a modulation of its phase and periodicity. The idea is that relatively small changes in the phase and period of the QBO, produced by solar activity, may significantly alter the wind field to produce a relatively large SCAE.

To investigate this hypothesis, we performed two modeling studies that led to different but complementary conclusions. In one we studied a hypothetical QBO with a period of 30 months, in the other one the period was close to 33 months. In both studies, the model was run with and without SCRV, and different source amplitudes and periods were employed. In case 1, the QBO period was stable and closely tied to the AO. In case 2, the QBO period was highly variable and therefore more susceptible to SCRV.

The first case study illustrates the SCAE associated with a QBO that has an unusually stable period. Without the ability to influence the phase and period of the QBO (see Fig. 4), the SCRV can only modulate the amplitude of the oscillation. As a result, the net effect of the SCRV is then relatively small. Considering the magnitudes of the variations imposed on the solar heating rates, however, the resulting differences in the modulated QBO amplitude are still significant. At mid-latitudes, there are no detectable signatures of the SCRV in the computed zonal wind fields—and this is in spite of the fact that the AO, directly generated by solar radiation, dominates at mid-latitudes.

The second case study has in common with the first that the equatorial oscillations, and the QBO in particular, are playing a central role in generating the solar activity effect in the middle atmosphere. But the dynamical situation here is different and to some extent more realistic. The QBO, having a period of about 33.5 months, is not tied as tightly to the seasonal forcing, so that its phase (and period) are much more amenable to the influence from solar activity variations. As shown in Fig. 8, the QBO period in this case is then highly variable with or without solar activity effects.

A complicating factor in the second case is that a beat period around 10 years is generated by the QBO as it interacts with the SAO through GW node filtering (Part I). The solar cycle variations with the same period can then be phase locked to this beat oscillation. This situation is apparent in Fig. 9a where the phase of the QBO gradually changes until, after about 7 years, it becomes locked in the opposite polarity (180° phase difference) to produce a large difference field. The phase of our hypothetical QBO also changes for the hypothetical 8-year activity cycle (Fig. 9b) but never locks into the state seen in Fig. 9a, although in later years the imposed phase difference becomes large enough to modify the QBO at lower altitudes. In this case, the difference field again reveals a periodicity around 10 years to reflect the solar activity effect, with amplitudes close to 20 m/s at altitudes around 60 km. The average period in the difference field (Fig. 10b) is not 8 years, and this indicates that the natural beat period of 10 years continues to play an important role.

In contrast to case 1 where the solar activity effect is confined to low latitudes, the effect extends to higher latitudes and is relatively large for the case study 2. Distinct variations are seen in the difference fields for both activity cycles (Fig. 11)—but it is not clear how they are generated. In a 2D model, the most likely explanation is that the meridional circulation is carrying the solar activity signature in the QBO towards higher latitudes. This has been suggested for the signature of the 10-year beat period (Part I) that appears also at mid latitudes although it is generated by the QBO that is confined to low latitudes. The zonal circulation of the QBO, whose amplitude and period are modulated by solar activity, can generate such a meridional circulation through the Coriolis force. And the long periods in the range of 10 years may be conducive to induce perturbations at lower altitudes where the time constants for radiative cooling and diffusion are long.

Our study samples are not representative of the real world, with the QBO of 30 months that is phase locked to the seasonal cycle, and the QBO of 33.5 months that is at the upper end of observed periodicities. The study was conducted with the 2D version of our model that permits integrations over periods of several decades. In 3D, planetary wave processes become important that could affect the outcome significantly.

Notwithstanding these limitations, we believe that our model study does illustrate how the wave-driven equatorial oscillations and the QBO in particular may affect and amplify the solar cycle variations in the middle atmosphere. Through downward control that involves the seasonal cycle, the QBO can act as a conduit of the solar cycle effect to lower altitudes that in turn amplifies it. Through seasonal variations and downward control, the period of the QBO is modulated and that in turn produces large solar activity signatures in the model.

Acknowledgements

This work was supported in part by the NASA Office of Space Science under NRA-98-03-ITM-080. The authors acknowledge discussions with Dr. Ken Schatten regarding a reasonable choice for the solar cycle variations in radiance, and they are indebted to two reviewers for valuable comments, both critical and clarifying, that helped to improve the paper.

References

Balachandran, N.K., Rind, D., 1995. Modeling the effects of UV variability and the QBO on the troposphere–stratosphere system. Part 1: The middle atmosphere. Journal of Climatology 8, 2058.

Balachandran, N.K., Rind, D., Lonergan, P., Shindell, D.T., 1999. Effects of solar cycle variability in the lower stratosphere and troposphere. Journal Geophysical Research 104, 22321.

Baldwin, M.P., Dunkerton, T.J., 1998. Biennial, quasi-biennial, and decadal oscillations of potential vorticity in the northern stratosphere. Journal of Geophysical Research 103, 3919.

Burrage, M.D., Vincent, R.A., Mayr, H.G., Skinner, W.R., Arnold, N.F., Hays, P.B., 1996. Long-term variability in the equatorial middle atmosphere zonal wind. Journal of Geophysical Research 101, 12847.

Chan, K.L., Mayr, H.G., Mengel, J.G., Harris, I., 1994. A 'stratified' spectral model for stable and convective atmospheres. Journal of Computational Physics 113, 165.

Dunkerton, T.J., 1979. On the role of the Kelvin wave in the westerly phase of the semiannual zonal wind oscillation. Journal of Atmospheric Science 36, 32.

Dunkerton, T.J., 1982a. Theory of the mesopause semiannual oscillation. Journal of Atmospheric Science 39, 2681.

Dunkerton, T.J., 1982b. Wave transcience in a compressible atmosphere. 3. The saturation of internal gravity waves in the mesosphere. Journal of Atmospheric Science 39, 1042.

Dunkerton, T.J., 1982c. Stochastic parameterization of gravity wave stresses. Journal of Atmospheric Science 39, 1711.

Dunkerton, T.J., 1985. A two-dimensional model of the quasi-biennial oscillation. Journal of Atmospheric Science 42, 1151.

Dunkerton, T.J., 1997. The role of gravity waves in the quasi-biennial oscillation. Journal of Geophysical Research 102, 26053.

Dunkerton, T.J., Baldwin, M.P., 1992. Modes of interannual variability in the stratosphere. Geophysical Research Letters 19, 49.

Dunkerton, T.J., Delisi, D.P., 1997. Interaction of the quasi-biennial oscillation and the stratopause semiannual oscillation. Journal of Geophysical Research 102, 26107.

Fritts, D.C., Lu, W., 1993. Spectral estimates of gravity wave energy and momentum fluxes: II, Parameterization of wave forcing and variability. Journal of Atmospheric Science 50, 3695.

Garcia, R.R., Dunkerton, T.J., Lieberman, R.S., Vincent, R.A., 1997. Climatology of the semiannual oscillation of the tropical middle atmosphere. Journal of Geophysical Research 102, 26014.

Hamilton, K., 1986. Dynamics of the stratospheric semi-annual oscillation. Journal of Meteorological Society of Japan 64, 227.

Hamilton, K., Wilson, R.J., Mahlman, J.D., Umscheid, L.J., 1995. Climatology of the SKYHI troposphere–stratosphere–mesosphere general circulation model. Journal of Atmospheric Science 52, 5.

Hines, C.O., 1997a. Doppler-spread parameterization of gravity-wave momentum deposition in the middle atmosphere. 1. Basic formulation. Journal of Atmospheric and Solar Terrestrial Physics 59, 371.

Hines, C.O., 1997b. Doppler-spread parameterization of gravity-wave momentum deposition in the middle atmosphere. 2. Broad and quasi monochromatic spectra, and implementation. Journal of Atmospheric and Solar Terrestrial Physics 59, 387.

Hirota, I., 1980. Observational evidence of the semiannual oscillation in the tropical middle atmosphere—a review. Pure and Applied Geophysics 118, 217.

Hitchman, M.H., Leovy, C.B., 1988. Estimation of the Kelvin wave contribution to the semiannual oscillation. Journal of Atmospheric Science 45, 1462.

Holton, J.R., Lindzen, R.S., 1972. An updated theory for the quasi-biennial cycle of the tropical stratosphere. Journal of Atmospheric Science 29, 1076.

Holton, J.R., Tan, H.C., 1980. The influence of the equatorial quasi-biennial oscillation on the global circulation, at 50 mb. Journal of Atmospheric Science 37, 2200.

Labitzke, K., 1982. On the interannual variability of the middle stratosphere during northern winters. Journal of Meteorological Society of Japan 60, 124.

Labitzke, K., 1987. Sunspots, the QBO and stratospheric temperature in the north polar region. Geophysical Research Letters 14, 135.

Labitzke, K., Van Loon, H., 1988. Association between the 11-year solar cycle, the QBO and the atmosphere. Part I: the troposphere and stratosphere in the northern hemisphere in winter. Journal of Atmospheric and Terrestrial Physics 50, 197.

Labitzke, K., Van Loon, H., 1992. On the association between the QBO and the extratropical stratosphere. Journal of Atmospheric and Terrestrial Physics 54, 1453.

Lindzen, R.S., 1981. Turbulence and stress due to gravity wave and tidal breakdown. Journal of Geophysical Research 86, 9707.

Lindzen, R.S., Holton, J.R., 1968. A theory of the quasi-biennial oscillation. Journal of Atmospheric Science 25, 1095.

Mayr, H.G., Mengel, J.G., Hines, C.O., Chan, K.L., Arnold, N.F., Reddy, C.A., Porter, H.S., 1997. The gravity wave Doppler spread theory applied in a numerical spectral model of the middle atmosphere. 2. Equatorial oscillations. Journal of Geophysics Research 102, 26093.

Mayr, H.G., Mengel, J.G., Chan, K.L., 1998. Equatorial oscillations maintained by gravity waves as described with the Doppler Spread Parameterization: I. numerical experiments. Journal of Atmospheric and Solar Terrestrial Physics 60, 181.

Mayr, H.G., Mengel, J.G., Reddy, C.A., Chan, K.L., Porter, H.S., 2000. Properties of the QBO and SAO generated by gravity waves. Journal of Atmospheric and Solar Terrestrial Physics 62, 1135.

Mayr, H.G., Mengel, J.G., Drob, D.P., Chan, K.L., Porter, H.S., 2001. Modeling studies with QBO: I. quasi decadal oscillation. Journal of Atmospheric and Solar Terrestrial Physics, submitted for publication.

Mengel, J.G., Mayr, H.G., Chan, K.L., Hines, C.O., Reddy, C.A., Arnold, N.F., Porter, H.S., 1995. Equatorial oscillations in the middle atmosphere generated by small scale gravity waves. Geophysical Research Letters 22, 3027.

Naito, Y., Hirota, I., 1997. Interannual variability of the northern winter stratospheric circulation related to the QBO and the solar cycle. Journal of Meteorological Society of Japan 75, 925.

Plumb, R.A., 1977. The interaction of two internal waves with the mean flow: implications for the theory of the quasi-biennial oscillation. Journal of Atmospheric Science 34, 1847.

Plumb, R.A., 1984. The quasi-biennial oscillation. In: Holton, J.R., Matsuna, T. (Eds.), Dynamics of the Middle Atmosphere. Terra Sci., Tokyo 217.

Plumb, R.A., Bell, R.C., 1982. A model of the quasi-biennial oscillation on an equatorial beta-plane. Quarterly Journal of the Royal Meteorological Society 108, 335.

Reed, R.J., 1965. The quasi-biennial oscillation of the atmosphere between 30 and 50 km over Ascension Island. Journal of Atmospheric Science 22, 331.

Reed, R.J., 1966. Zonal wind behavior in the equatorial stratosphere and lower mesosphere. Journal of Geophysical Research 71, 4223.

Salby, M., Callaghan, P., 2000. Connection between the solar cycle and the QBO: the missing link. Journal of Climatology 13, 2652.

Soukharev, B.E., Hood, L.L., 2001. Possible solar modulation of the equatorial quasi-biennial oscillation: additional statistical evidence. Journal of Geophysical Research 106, 14855.

Strobel, D.F., 1978. Parameterization of atmospheric heating rate from 15 to 120 km due to O2 and O3 absorption of solar radiation. Journal of Geophysical Research 83, 7963.

Takahashi, M., 1999. Simulation of the quasi-biennial oscillation in a general circulation model. Geophysical Research Letters 26, 1307.

Takahashi, M., Boville, B.A., 1992. A three-dimensional simulation of the equatorial quasi-biennial oscillation. Journal of Atmospheric Science 49, 1020.

Van Loon, H., Labitzke, K., 1993. Review of the decadal oscillation in the stratosphere of the northern hemisphere. Journal of Geophysical Research 98, 18919.

Van Loon, H., Labitzke, K., 1998. The global range of the stratospheric decadal wave. Part I: its association with the sunspot cycle in summer and in the annual mean, and with the troposphere. Journal of Climatology 11, 1529.

Wehrbein, W.M., Leovy, C.B., 1982. An accurate radiative heating and cooling algorithm for use in a dynamical model of the middle atmosphere. Journal of Atmospheric Science 39, 1532.

Zhu, X., 1989. Radiative cooling calculated by random band models with S-1-beta tailed distribution. Journal of Atmospheric Science 46, 511.